ON THE SIMILARITIES OF THE ENGINEERING AND ATMOSPHERIC BOUNDARY LAYERS

Guillermo Araya[1], L. Castillo[1], A. Ruiz-Columbie[2], J. Schroeder[3], and S. Basu[4]

[1]Department of Mechanical Engineering, National Wind Resource Center, Texas Tech University, Lubbock, TX, 79409, USA

[2]University College, Texas Tech University, Lubbock, TX, 79409, USA

[3]Atmhosperic Science, Texas Tech University, Lubbock, TX, 79409, USA

[4]Department of Marine, Earth, and Atmospheric Sciences, North Carolina State University, Raleigh, NC 27695, USA

ABSTRACT

In this study, a comparison of different turbulent flow parameters is performed between a spatially-developing boundary layer (SDBL) and the corresponding atmospheric boundary layer (ABL). Numerical data for the SDBL have been obtained by performing Direct Numerical Simulations (DNS) at different Reynolds numbers and stream-wise pressure gradients. Turbulent inflow conditions have been generated by means of the dynamic multi-scale approach (Araya *et al*., 2011). On the other hand, observational data for the ABL are available for the comparison. The idea is to test and validate the extension of the engineering scaling laws to the real ABL. Those scaling laws have been developed by carrying out a similarity analysis over the governing equations of the flow (George & Castillo 1997, Wang & Castillo 2003).

Keywords: DNS, thermal boundary layer, SDBL, ABL, stratification, inflow conditions.

1. INTRODUCTION

Transport of passive scalars in turbulent flows plays a key role in many engineering applications such as wind energy, electronic cooling, combustion and turbine-blade film cooling, as well as in atmospheric flows. Examples of passive scalars are temperature, humidity, pollutants, or any other chemical species. In addition, a passive scalar is a diffusive additive that possesses no dynamical effect on the flow motion because of its low concentration. A comprehensive review about passive scalars can be found in Sreenivasan (1991), Sreenivasan *et al*. (1977); and, more recently, in the study carried out by Warhaft (2000). Furthermore, the concept of passive scalars and thermal fields is equivalent only under specific assumptions. Hence, if the temperature difference in the thermal boundary layer is assumed small, the buoyancy effects and temperature dependence of material properties are negligible. As a consequence, the temperature may be considered as a passive scalar, and the momentum and the heat transfer equations are uncoupled. Moreover, in the past, the problem of heat transfer has been principally investigated by means of experiments to explore the temperature as a passive scalar. On the other hand, if the temperature difference is significant, buoyancy cannot be neglected and the boundary layer is considered to be under stratification. Furthermore, thermal stratification occurs when the high temperature variations provoke fluid separation due to buoyant forces.

Moreover, direct simulations (DNS) have tried to shed some light on the transport phenomena, particularly in the near-wall region

Corresponding author: G. Araya (araya@mailaps.org)

of boundary layers where most of the experimental techniques have limitations due to the spatial resolution. Most of the DNS of passive scalars known so far have been performed on fully developed turbulent channels, in which periodic boundary conditions in the streamwise direction can be applied (Kim and Moin (1989) and Kasagi and Iida (1999)). However, in the simulations of turbulent spatially-developing boundary layers, the periodic boundary condition cannot be prescribed because the flow is developing in the streamwise direction. Hence, the appropriate instantaneous velocity and temperature profiles must be imposed at the inflow for each time step. Lund *et al*. (1998), referred henceforth as LWS, have proposed a methodology to generate the inlet velocity profile based on the solution downstream by assuming self-similarity of the flow in the streamwise direction. LWS tested the proposed method by performing Large Eddy Simulations (LES) in zero pressure gradient flows, and the range for the momentum thickness Reynolds number, Re_θ , was 1530 – 2150.

To the best of our understanding, there are only a few numerical simulations of spatially-evolving thermal boundary layers in ZPG flows. Bell and Ferziger (1993) used a modified version of Spalart's code, which considered the "fringe" concept to convert the non-periodic conditions into periodic ones (Spalart and Watmuff (1993)). In their study, direct simulations were performed in iso-scalar walls for an extent of momentum thickness Reynolds number from 300 to 700 and values of the Prandtl number equal to 0.1, 0.71, and 2.0. They concluded that the momentum and passive scalar fields at Pr = 0.71 were highly correlated in the near wall region. Kong *et al*. (2000) extended the rescaling-recycling method by LWS to generate time-dependant inflow thermal information in direct simulations of turbulent boundary layers in ZPG flows. The momentum thickness Reynolds number range was 300 – 420. As in LWS, a single scale was considered along the entire boundary layer for the rescaling processes of the thermal field: the friction temperature, Θ_τ . Li *et al*. (2009) carried out DNS of a spatially developing turbulent boundary layer over a flat plate with the evolution of several passive scalars (Prandtl numbers = 0.2, 0.71, and 2) under both isoscalar and isoflux wall boundary conditions; the highest Re_θ was 830. They focused on the behavior of the scalars in the outer region of the boundary layer, which was significantly different from a channel-flow simulation. More recently, Wu & Moin (2010) have reported DNS of an incompressible ZPG thermal boundary layer with isothermal wall conditions. The range for the momentum thickness Reynolds numbers, Re_θ, was 80 - 1950 and the molecular Prandtl number Pr = 1. Furthermore, the DNS studies of turbulent thermal spatially-evolving boundary layers mentioned so far have involved ZPG flows. To the best of our knowledge and based on extensive literature review, published data on thermal DNS of pressure gradient flows are very limited (Araya & Castillo (2012)). Speaking about stratified flows, Hattori et al. (2007) employed the inflow generation method by Lund et al. (1998) and Kong et al. (2000) to investigate the effects of buoyancy on the near-wall region of stable and unstable turbulent thermal boundary layers. Furthermore, Hattori et al. (2007) performed direct simulations in the approximate range of 1000–1250 for Re_θ and concluded that thermal stratifications caused by the weak buoyant force significantly altered the structure of near-wall turbulence.

In this paper, an innovative Dynamic Multi-scale method for generation of inflow turbulent thermal information is presented based on the work carried out by Lund *et al*. (1998) and Kong *et al*. (2000). The scaling laws are obtained by performing a similarity analysis over the governing equations in the inner and outer regions of the boundary layer. The velocity scaling is based on the analysis performed by George and Castillo (1997) and successfully implemented by Araya (2008), Araya *et al.* (2009) and Araya *et al.* (2011) in turbulent velocity boundary layers at zero and adverse and favorable pressure gradients. The temperature scales were developed according to investigations performed by Wang and Castillo (2003). The principal contributions of the proposed inflow generation technique can be summarized as follows: i) the consideration of different scaling laws in the inner and outer zones of the boundary layer permits the assimilation of streamwise pressure gradients, such as APG, and ii) the implementation of a dynamic approach to compute inlet parameters at each time step (necessary during the rescaling process) based on the solution downstream, this avoids the use of empirical correlation as in LWS, so that more general flows can be simulated. Additionally, low and high order statistics from present DNS of passive scalars are compared with experimental and numerical data from the literature. Finally, the SDBL results are contrasted against observational data (ABL) from the 200m Met Tower located at Texas Tech University in order to assess the collapsing properties of the proposed scaling laws.

2. DESCRIPTION OF THE MULTI-SCALE METHOD

Figure 1 shows a schematic of the thermal boundary layer with the inner and outer regions. The recycle plane is conveniently located far downstream from the inlet in order to ensure an almost zero value for the two-point correlation of any flow variable between these two planes. However, the selection of the recycle plane location is a trade off: the further the distance between inlet and recycle planes, the longer the time for reaching equilibrium on flow parameters between these two planes; as a consequence, the transient time is penalized. The main improvement in this study is the utilization of two different scaling laws in the inner and outer parts of the boundary layer and a test plane. Table 1 shows the proposed scaling laws used for the momentum and thermal boundary layers as well as the single scaling approach employed by Lund *et al.* (1998) and Kong *et al.* (2000). The velocity and thermal scaling laws are obtained by performing a multi-scale similarity analysis of the governing equations. Further details about the development of the proposed scaling laws and the procedure for turbulent inflow generation can be found in Araya (2008).

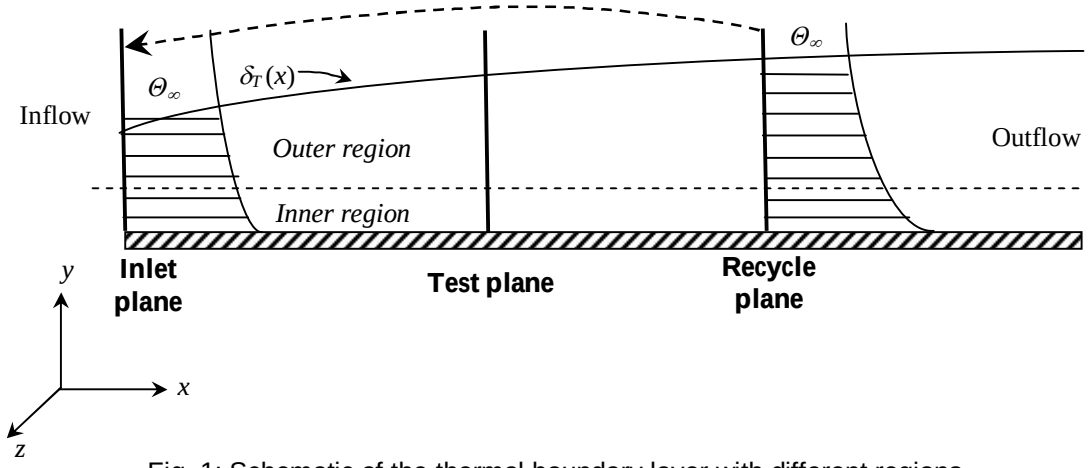

Fig. 1: Schematic of the thermal boundary layer with different regions.

Table 1: Velocity and temperature scaling.

Parameter	Type	Single scaling		Proposed scaling	
		Inner	Outer	Inner	Outer
U	Mean velocity along x	u_τ	u_τ	u_τ	U_∞
V	Mean velocity along y	U_∞	U_∞	u_τ	$U_\infty \frac{d\delta}{dx}$
u'	Fluctuating velocity along x	u_τ	u_τ	u_τ	U_∞
v'	Fluctuating velocity along y	u_τ	u_τ	u_τ	$U_\infty \frac{d\delta}{dx}$
$\overline{\Theta}$	Mean temperature	Θ_τ	Θ_τ	$\mathrm{Pr}\sqrt{S_t}(\Theta_w - \Theta_\infty)$	$(\Theta_w - \Theta_\infty)\frac{\delta_T^*}{\delta_T}$
θ'	Fluctuating temperature	Θ_τ	Θ_τ	$\mathrm{Pr}\sqrt{S_t}(\Theta_w - \Theta_\infty)$	$(\Theta_w - \Theta_\infty)\frac{\delta_T^*}{\delta_T}$

The instantaneous temperature is expressed as a contribution of a mean value plus a fluctuation. Furthermore, in the inner region the mean temperature follows a thermal law of the wall given as,

$$\Theta_w - \overline{\Theta}^{inner} = T_{si}(x) g_{si\infty}(y_T^+, \mathrm{Pr}, *) \quad (1)$$

where * accounts for any upstream effects. In the outer region, a defect law is applied,

$$\overline{\Theta}^{outer} - \Theta_\infty = T_{so}(x) g_{so\infty}(\bar{y}_T, \mathrm{Pr}, *) \quad (2)$$

Notice that $T_{si}(x)$ and $T_{so}(x)$ are the unknown

temperature scales for the inner and outer layers and only depend on x. Applying eqns. (1) and (2) to the inlet and recycle planes and assuming that functions $g_{si\infty}(y_T^+, \mathrm{Pr}, *)$ and $g_{so\infty}(\bar{y}_T, \mathrm{Pr}, *)$ are the same at both streamwise stations in the limit as $\delta^+ = \delta u_\tau / \upsilon \to \infty$,

$$\overline{\Theta}_{inl}^{inner} = \lambda_{Ti}\,\overline{\Theta}_{rec} + \Theta_{w,inl} - \lambda_{Ti}\Theta_{w,rec} \quad (3)$$

$$\overline{\Theta}_{inl}^{outer} = \lambda_{To}\,\overline{\Theta}_{rec} + (1-\lambda_{To})\Theta_{\infty} \quad (4)$$

The λ_T-parameters are the ratios of the mean temperature scales at the inlet and at the recycle planes, for inner and outer zones, respectively,

$$\lambda_{Ti} = \frac{T_{si,inl}}{T_{si,rec}} = \frac{\left[\mathrm{Pr}\sqrt{S_t}\left(\Theta_w - \Theta_\infty\right)\right]_{\mathrm{inl}}}{\left[\mathrm{Pr}\sqrt{S_t}\left(\Theta_w - \Theta_\infty\right)\right]_{\mathrm{rec}}} = \frac{\left[\sqrt{S_t}\left(\Theta_w - \Theta_\infty\right)\right]_{\mathrm{inl}}}{\left[\sqrt{S_t}\left(\Theta_w - \Theta_\infty\right)\right]_{\mathrm{rec}}} \quad (5)$$

$$\lambda_{To} = \frac{T_{so,inl}}{T_{so,rec}} = \frac{\left[\left(\Theta_w - \Theta_\infty\right)\dfrac{\delta_T^*}{\delta_T}\right]_{\mathrm{inl}}}{\left[\left(\Theta_w - \Theta_\infty\right)\dfrac{\delta_T^*}{\delta_T}\right]_{\mathrm{rec}}} \quad (6)$$

The definitions of all terms can be found in the Nomenclature section. Moreover, a similar procedure is used for the temperature fluctuations in the inner and outer regions,

$$\theta'^{inner} = T'_{si}(x)\,g'_{si\infty}(y_T^+, z_T^+, \bar{t}_{si}) \quad (7)$$

$$\theta'^{outer} = T'_{so}(x)\,g'_{so\infty}(\bar{y}_T, \bar{z}_T, \bar{t}_{so}) \quad (8)$$

Hence, the fluctuations at inlet can be obtained from those at the recycle location,

$$\theta'^{inner}_{inl}(y^+_{T,inl}, z_T^+, \bar{t}_{si}) = \lambda'_{Ti}\,\theta'_{rec}(y^+_{T,inl}, z_T^+, \bar{t}_{si}) \quad (9)$$

$$\theta'^{outer}_{inl}(\bar{y}_{T,inl}, \bar{z}_T, \bar{t}_{so}) = \lambda'_{To}\,\theta'_{rec}(\bar{y}_{T,inl}, \bar{z}_T, \bar{t}_{so}) \quad (10)$$

It was found in Araya and Castillo (2012) that $\lambda_{Ti} = \lambda'_{Ti}$ and $\lambda_{To} = \lambda'_{To}$. Furthermore, a composite profile can be expressed in the entire thermal boundary layer by defining a weighted average of the inner and outer profiles,

$$\Theta = \left[\overline{\Theta}_{inl}^{inner} + \theta'^{inner}_{inl}\right]\left[1 - W(\bar{y}_{T,inl})\right] + \left[\overline{\Theta}_{inl}^{outer} + \theta'^{outer}_{inl}\right] W(\bar{y}_{T,inl}) = \overline{\Theta}_{inl} + \theta'_{inl} \quad (11)$$

where the weight function, $W(\bar{y}_T)$, is defined as,

$$W(\bar{y}_T) = \frac{1}{2}\left[1 + \tanh\left(\frac{a\,(\bar{y}_T - b)}{(1-2b)\bar{y}_T + b}\right)\Big/\tanh(a)\right] \quad (12)$$

In the Lund's method, the selected values for *a* and *b* after performing an analysis on independent spatially evolving boundary layer were *a* = 4 and $b = 0.2$ and also used in this investigation.

The ratios λ_{Ti} and λ_{To}, given by expressions (5) and (6), require the values of S_t, $\left(\Theta_w - \Theta_\infty\right)$, δ_T and δ_T^* at the inlet and recycle planes. For the Stanton number at both stations (i.e., the inlet and recycle planes) the following equation is employed, which was developed by matching the inner and outer profiles in the overlap region, Wang *et al*. (2008),

$$S_t = \left[\frac{1}{\mathrm{Pr}}\frac{\delta_T^*}{\delta_T}\left(-\frac{C_{oT\infty}}{C_{iT\infty}}\right)\exp\left[\frac{A}{\left(\ln\delta_T^+\right)^\alpha}\right]\left(\delta_T^+\right)^{-\gamma_{T\infty}}\right]^2 \quad (13)$$

Furthermore, the mean temperature profile was prescribed during the transient period to guide

the thermal field and only the fluctuations were rescaled from the recycle plane. The imposed mean temperature during the transient at the inlet plane was based on the composite profile by Wang and Castillo (2003). Moreover, the thermal boundary layer thickness at inlet, $(\delta_T)_{inl}$, is fixed as in the velocity field. The boundary layer thickness at the recycle plane and thermal displacement thicknesses at both planes are computed from the mean temperature profiles. This procedure was observed to produce accurate and stable results with a short thermal transient.

3. THE DYNAMIC APPROACH

We concern ourselves with simulating a thermal boundary layer as shown in the schematic in figure 1. Thermal turbulent inflow information is required at the inlet plane. The Cartesian coordinates *x*, *y* and *z* denote the streamwise, wall-normal and spanwise directions, respectively. The flow is divided into inner and outer regions. Also, the instantaneous temperature Θ is decomposed into a mean value $\overline{\Theta}$ and a fluctuation θ'. The basic idea of the rescaling–recycling method of LWS is to construct a time-dependent velocity field at the inlet separately in the inner and outer regions, according to equation (11). For the inner region, the ratio of friction velocities, u_τ, at the inlet to the recycle planes must be specified. While the stress may be measured near the wall at the recycle station, the stress at the inlet is unknown. In LWS. this problem was overcame by invoking an empirical law describing the evolution with downstream Reynolds number, i.e. taking the ratio of friction velocities to be equal to $(\theta_{rec}/\theta_{inl})^{1/8}$, where 1/8 comes from the usual '1/n' power-law exponent of boundary layers and θ is the momentum thickness computed through the mean velocity. Nevertheless, since the 1/8 power is greatly impacted by pressure gradients and other effects such as possibly wall roughness and free-stream turbulence and also weakly by the Reynolds number, it is not justified to use 1/8 in all cases. Therefore, this formulation for computing the friction velocity ratio is limited in principle to ZPG flows. In order to extend the rescaling-recycling method to more general flows besides the canonical boundary layer flows, Araya *et al*. (2011) introduced a dynamic approach to calculate this power based on the flow solution downstream,

$$u_\tau / U_\infty \sim \left(\mathrm{Re}_\delta\right)^\gamma \tag{14}$$

by invoking a new plane between the inlet and recycle stations, called the test plane, as seen in figure 1. The reader is referred to Araya *et al*. (2011) for further details on the dynamic method for the velocity boundary layer. In this section, we are briefly describing the corresponding dynamic thermal approach, as implemented in Araya *et al*. (2012). It is assumed a power law of the thermal boundary layer thickness Reynolds number for the friction temperature, as follows;

$$\Theta_\tau / \Theta_\infty \sim \left(\mathrm{Re}_{\delta_T}\right)^{\gamma_T} \tag{15}$$

For scaling purposes, the ratio of the friction temperatures at the inlet to the recycle planes are needed,

$$\frac{\left(\Theta_\tau/\Theta_\infty\right)_{inl}}{\left(\Theta_\tau/\Theta_\infty\right)_{rec}} = \left(\frac{\mathrm{Re}_{\delta_T\ inl}}{\mathrm{Re}_{\delta_T\ rec}}\right)^{\gamma_T} \tag{16}$$

Therefore, by considering the power law (15) at the test to the recycle planes, the unknown

power, γ_T, can be computed from the flow mean solution:

$$\gamma_T = \frac{\ln\left[\left(\Theta_\tau/\Theta_\infty\right)_{test}/\left(\Theta_\tau/\Theta_\infty\right)_{rec}\right]}{\ln\left(\mathrm{Re}_{\delta_T\ test}/\mathrm{Re}_{\delta_T\ rec}\right)} \qquad (17)$$

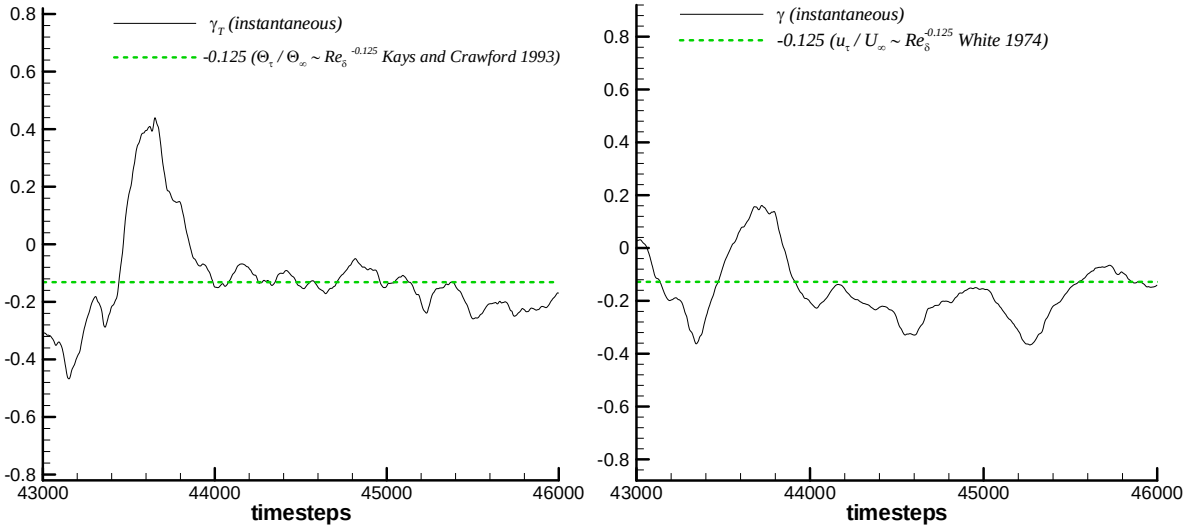

Fig. 2: Time variation of coefficients γ and γ_T in zero pressure gradient (ZPG) flows.

Figure 2 shows the time variation of the corresponding powers for the friction velocity (a) and the friction temperature (b) in ZPG flows at high Reynolds numbers. It is observed that the computed online powers oscillate around the proposed empirical correlations by Kays and Crawford (1993) and White (1974). Thus, once the powers are computed, the friction velocity and temperature can be calculated for any type of pressure gradient imposed.

4. NUMERICAL MODEL

The physical domain and the corresponding boundary conditions are shown in fig. 3. For the thermal field, an isothermal condition at the wall is considered. The no-slip condition is prescribed for the velocity components at the wall. Periodic boundary conditions are assumed in the spanwise direction for both fields. The pressure is prescribed at the exit plane. At the upper surface of the computational box, Dirichlet conditions are imposed for the streamwise velocity and temperature; moreover, the stress-free condition is set for the vertical and spanwise components of the velocity. For adverse and favorable pressure gradient cases (APG and FPG), the top surface is not flat as in the ZPG case. Therefore, a desired curvature is prescribed on the mesh in such a way to resemble a streamline.

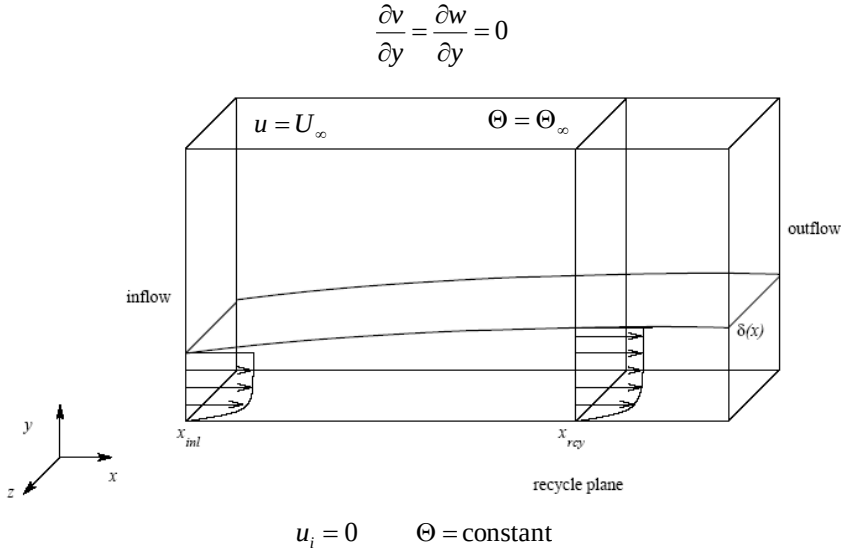

Fig. 3: Schematic of the physical domain in ZPG flow computations

Information about the domain dimensions, mesh configuration and input parameters are depicted by Table 2. In all cases, the boundary layer thickness, δ_{inlet}, at the inlet domain is fixed during the entire simulation. The incompressible version of PHASTA code (Parallel Hierarchic Adaptive Stabilized Transient Analysis) developed at RPI is used, which considers a Finite Element approach with a SUPG (Streamline Upwind Petrov-Galerkin) stabilization. It has been shown (Whiting and Jansen (2001)) to be an effective tool for bridging a broad range of length scales in turbulent (RANS, LES, DES, DNS) flows.

Table 2: Parameters of the different cases considered without stratification.

	ZPG		FPG	APG	
Parameter	Low Re_θ	High Re_θ	Moderate	Moderate	Strong
Re_θ	308–385	2667–3005	700	438–633	1029–1512
L_x/δ_{inl}	10.7	10	15	15	12
L_y/δ_{inl}	3	3	3	3.8	3
L_z/δ_{inl}	1.7	1.6	3	1.6	3.2
$N_x N_y N_z$	$90 \times 50 \times 40$	$400 \times 150 \times 125$	$200 \times 120 \times 120$	$120 \times 65 \times 50$	$150 \times 90 \times 100$
Δx^+	18.9	20	20	20	21
$\Delta y^+_{min}/\Delta y^+_{max}$	0.5/13	0.5/20	0.2/15	0.2/6.8	0.2/17
Δz^+	6.77	10	8	5	8
Δt^+	0.63	0.44	0.36	0.59	0.22
$T_{sample}\frac{u_\tau^2}{\nu}$	1890	2200	1080	1770	1540
δ^+_{inl}	152	980	446	161	271

5. RESULTS AND DISCUSSION

In this section, the numerical predictions obtained from the different cases considered without stratification, as seen in Table 2, are shown and discussed. Figure 4 illustrates the mean temperature profiles of all cases by considering the Wang-Castillo scaling (a) employed in the present investigation and the classical deficit coordinates (b). It is observed that all thermal profiles at different streamwise pressure gradients collapse by using the Wang-Castillo thermal scaling. However, the level of collapse given by the classical deficit law is very poor. Furthermore, a key factor in the rescaling-recycling approach is the utilization of scaling laws that are able to absorb external conditions such as pressure gradients or different Reynolds numbers.

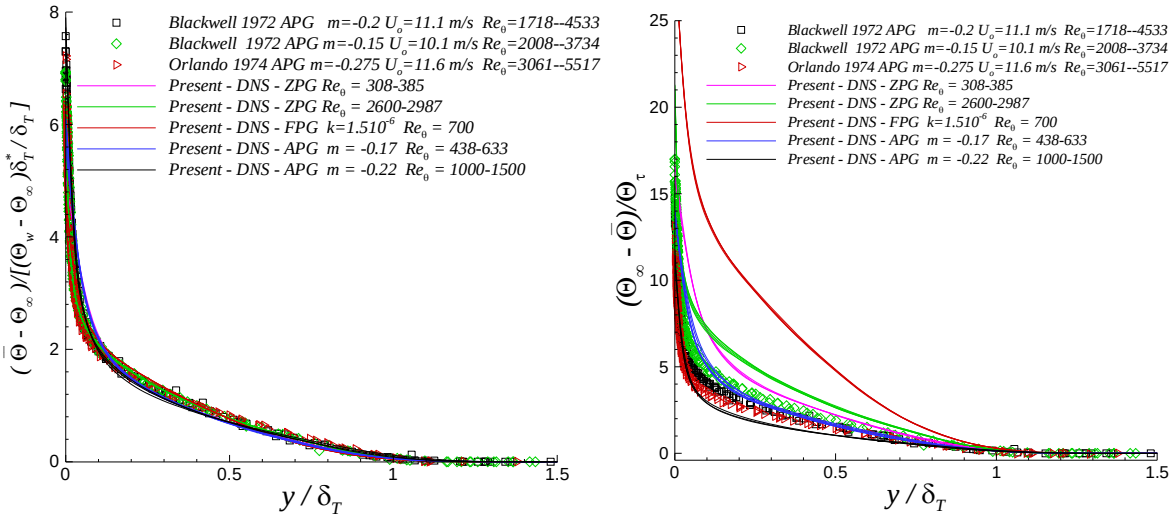

a) Wang-Castillo scaling. b) Classical scaling.

Figure 4: Mean temperature in outer coordinates.

In figure 5, the streamwise velocity fluctuations, u'^{+}_{rms}, and thermal fluctuations, θ'^{+}_{rms}, are shown for the ZPG, Moderate FPG and Strong APG cases. The idea is to analyze the effects of the Reynolds number and pressure gradient on the velocity and thermal fluctuations. For ZPG flows at low and high Reynolds numbers, there is a high similitude between streamwise velocity and thermal fluctuations for each case. Nevertheless, this correlation between u'^{+}_{rms} and θ'^{+}_{rms} completely disappears when a FPG or APG is imposed. Additionally, the peak or "shoulder" observed in the u'^{+}_{rms} profile for the Case APG at $y/\delta \approx 0.7$, it is not seen in the corresponding θ'^{+}_{rms} profile. Another important observation is given by the fact that streamwise velocity and thermal fluctuations show its maximum value closer to the wall as the Reynolds number increases when plotted in outer coordinates.

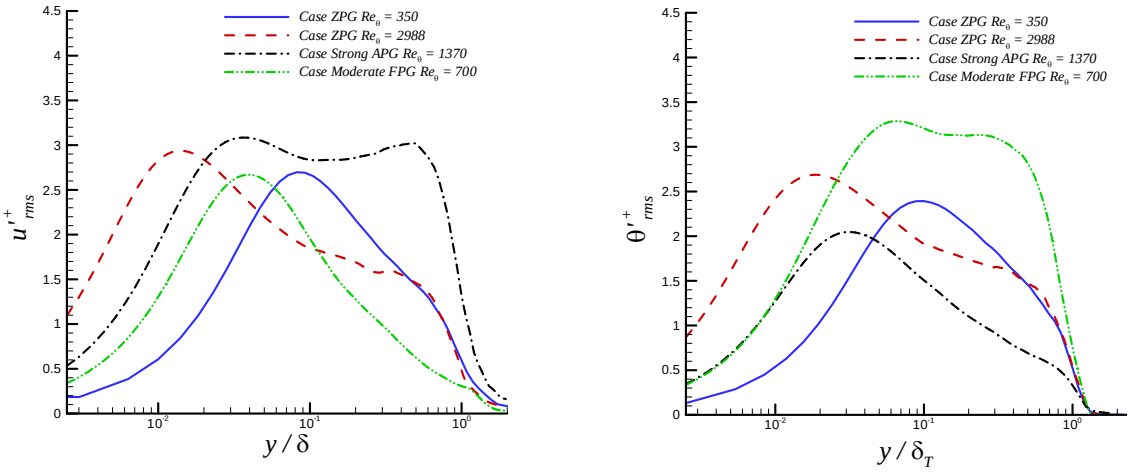

a) Streamwise velocity fluctuations. b) Thermal fluctuations.

Figure 5: Effects of Reynolds numbers and pressure gradient on thermal fluctuations.

The effects of pressure gradient on the temperature variance budget are also examined. The corresponding transport equation of the temperature variance, $\overline{\theta'^{+2}}/2$, reads:

$$\underbrace{-U_i^{+}\frac{\partial\left(\theta'^{+2}/2\right)}{\partial x_i^{+}}}_{Convection}\underbrace{-\overline{u_i'^{+}\theta'^{+}}\frac{\partial\overline{\Theta}^{+}}{\partial x_i^{+}}}_{\Pr oduction}\underbrace{-\frac{1}{2}\frac{\partial\left(\overline{\theta'^{+2}u_i'^{+}}\right)}{\partial x_i^{+}}}_{Turbulent\ \ diffusion}\underbrace{+\frac{1}{\Pr}\frac{\partial^2\left(\theta'^{+2}/2\right)}{\partial x_i^{+2}}}_{Molecular\ \ diffusion}\underbrace{-\frac{1}{\Pr}\overline{\frac{\partial\theta'^{+}}{\partial x_i^{+}}\frac{\partial\theta'^{+}}{\partial x_i^{+}}}}_{Dissipation}=0 \quad (18)$$

Figure 6 exhibits the different terms of eq. (18) close to the wall for the ZPG low Re_θ, Moderate APG and Moderate FPG cases. It can be appreciated that the peak value of $\overline{\theta'^{+2}}/2$ production in the buffer layer is not significantly influenced by the prescription of streamwise pressure gradient in the flow. However, the peak location is greatly modified. In the APG flow the peak of production is closer to the wall, while the peak location moves further from the wall in the FPG flow. Furthermore, the peak production in the ZPG flow adopts an intermediate location between the peak for APG and FPG cases. In addition, a similar trend is observed for the peak of the turbulent diffusion at $y^+ <$ 10. The imposition of an APG on the flow provokes an increase of the wall value for the molecular diffusion of $\overline{\theta'^{+2}}/2$ followed by an increase of the local peak at $y^+ \sim 7$, as well.

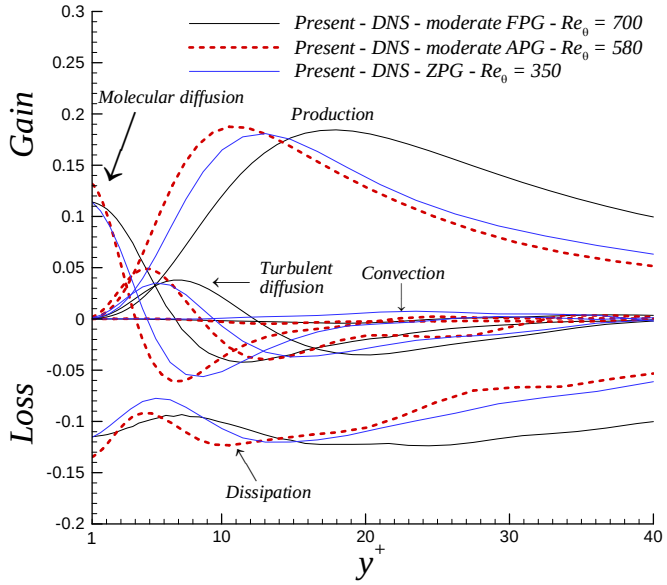

Fig. 6: Budget of the temperature variance in ZPG, APG and FPG flows.

5.1 COMPARISON WITH OBSERVATIONAL DATA

As mentioned above, ABL observational data from the West Texas Mesonet (WTM) 200-m tower were used in conjunction with Amarillo and Midland radiosounding data (Skew-T) to test and validate these engineering scaling laws. WTM is an independent project at Texas Tech University, with headquarters located at the Reese Center, about 12 miles West of Lubbock, Texas. Its 200-m tower takes 50-Hz observations of meteorological state variables, i.e. temperature and humidity, and also the

three wind components, at ten different height levels. Data corresponding to May 1st, 2012 were collected in order to create our case study. Additionally, the radiosoundings of that day from Amarillo and Midland, Texas, were used to determine the top heights of the boundary layer over Reese at the times of interest using spatial interpolation. Figure 7 shows the mean temperature profiles in outer scaling (Wang-Castillo) of present DNS, experimental data from Blackwell (1972) and Orlando (1974). Additionally, observational data from the Mesonet are also included at three different hours: 5:00AM, 8:30AM and 1:30PM, which corresponds to stable, neutral and unstable conditions. The collected sample consists of 90,000 points saved every 0.02 sec. (50Hz). It can be observed that only the stable atmospheric boundary layer collapses to the rest of the data (without stratification). Ongoing analysis is being conducted to develop new scaling laws that should be able to absorb buoyancy and stratifications effects, particularly, based on the Richardson number.

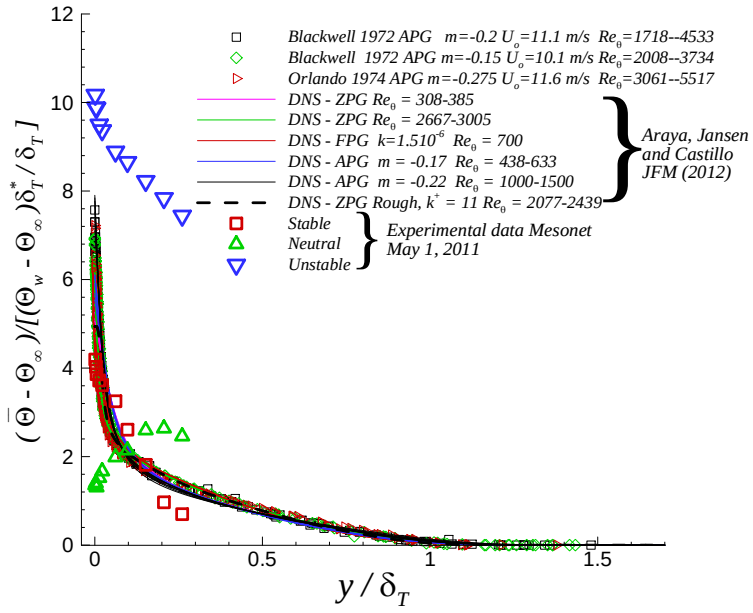

Figure 7: Corresponding ABL calculations on the Wang-Castillo Scaling

It is important to point out that the collapse of stable conditions into the engineering scaling seems to deteriorate with heights approximately at the top of the inner layer. We hypothesize that uncertainties in the determination of the top height of the boundary layer might contribute to it, although also the presence of weather conditions that day may be the main cause of such a disagreement because mesoscale and synoptic conditions appear to have a greater impact at higher altitudes in the ABL. More

case studies are needed in order to obtain a more accurate statement on this matter.

6. CONCLUSIONS

Extensive direct simulations (DNS) of spatially-evolving hydrodynamic and thermal boundary layers have been performed at low/high Reynolds numbers and for zero, favorable and adverse streamwise pressure gradients. A dynamic multi-scale method for generation of turbulent inflow information at the domain inlet is presented in this paper based on the rescaling-recycling method by LWS. The velocity scaling is based on the studies by George and Castillo (1997) and, the temperature scales were developed based on investigations performed by Wang and Castillo (2003).

The rescaling-recycling method has been shown to possess great capabilities as turbulent inflow generator in the simulations of momentum/thermal spatially-evolving boundary layers. Furthermore, the innovative approach has produced satisfactory results in zero, favorable and adverse pressure gradient flows. Numerical simulations are in fairly good agreement with other numerical data and empirical correlations from the literature. The major effect of adverse pressure gradient on flow parameters has been identified as a local peak, particularly on streamwise velocity fluctuations, in the outer region. However, this peak was not observed on thermal fluctuations. Furthermore, as the Reynolds number increases, the location of the maximum thermal fluctuations moved closer to the wall when plotted in outer coordinates. Furthermore, all DNS results for the mean temperature in outer Wang-Castillo scaling collapsed in a single curve, demonstrating the capabilities of this scaling law to absorb the effects of different Reynolds numbers and streamwise pressure gradients in thermal boundary layers without stratification. Finally, only the stable condition for the observational data from the Mesonet tower collapsed to the DNS results by using the Wang-Castillo scaling.

7. REFERENCES

Araya, G. 2008 DNS of turbulent wall bounded flows with a passive scalar. PhD thesis, Rensselaer Polytechnic Institute, Troy, NY.

Araya G., Jansen K. and Castillo L., Inlet condition generation for spatially-developing turbulent boundary layers via multi-scale similarity, Journal of Turbulence, 10, No. 36, pp. 1-33, 2009.

Araya G., Castillo L., Meneveau C. and Jansen K., A dynamic multi-scale approach for turbulent inflow boundary conditions in spatially evolving flows, Journal of Fluid Mechanics vol. 670, pp. 581–605, 2011.

Araya G. and Castillo L., DNS of turbulent thermal boundary layers up to Re_θ = 2300, Int. Journal of

Heat and Mass Transfer, Volume 55, Issues 15–16, 4003-4019, 2012.

Araya G., Jansen K. and Castillo L., DNS of turbulent thermal boundary layers subjected to streamwise pressure gradients, under consideration of the J. of Fluid Mechanics, 2012.

Bell D. M. and Ferziger J. H., Turbulent boundary layer DNS with passive scalars, In Near-Wall Turbulent Flows, edited by R. M. C. So, C. G. Speziale, and B. E. Launder (Elsevier, Amsterdam) pp. 327–336 (1993).

Blackwell B., The turbulent boundary layer on a porous plate: An experimental study of the heat transfer behavior with adverse pressure gradients, PhD Dissertation, Stanford University, 1972.

George W. K. and Castillo L., Zero-pressure-gradient turbulent boundary layer. Appl. Mech. Rev. 50, 689-729 (1997).

Hattori H., Houra T. and Nagano Y., Direct numerical simulation of stable and unstable turbulent thermal boundary layers, Int. Journal of Heat and Fluid Flow 28 1262–1271 (2007).

Kasagi N. and Iida O., Progress in direct numerical simulation of turbulent heat transfer, In Proceedings of the 5th ASME/JSME Thermal Engineering Joint Conference (1999).

Kays W. M. and Crawford M. E., *Convective Heat and Mass Transfer*, 3rd ed., McGraw–Hill, New York, 1993.

Kim J., Moin P., Transport of passive scalars in a turbulent channel flow, Turbulent Shear Flows, vol. 6. Springer, Berlin, pp. 85–96 (1989).

Kong H., Choi H. and Lee J., Direct numerical simulation of turbulent thermal boundary layers, Phys. of Fluids 12, 2555-2568 (2000).

Li Q., Schlatter P., Brandt L., Henningson D., DNS of a spatially developing turbulent boundary layer with passive scalar transport, International Journal of Heat and Fluid Flow 30, 916–929, 2009.

Lund T. Wu X. and Squires K., Generation of turbulent inflow data for spatially-developing boundary layer simulations, J. Comput. Phys. 140, 233-258 (1998).

Orlando A. F., Kays W. M. and Moffat R. J., Turbulent transport of heat and momentum in a boundary layer subject to deceleration, suction, and variable wall temperature. Report HMT-17, Thermosciences Division, Dep. of Mechanical Eng., Stanford University, 1974.

Spalart P.R. and Watmuff, J.H., Experimental and numerical study of a turbulent boundary layer with pressure gradients, J. Fluid Mech. 249 337–371 (1993).

Sreenivasan KR, On local isotropy of passive scalars in turbulent shear flows, Proc. R. Soc. London. Series A 434:165–82 (1991).

Sreenivasan K.R., Antonia R.A., Danh H.Q., Temperature dissipation fluctuations in a turbulent boundary layer, Phys. Fluids 20:1238–49 (1977).

Wang X., Castillo L., Asymptotic solutions in forced convection turbulent boundary layers, J. of Turbulence 4, pp.1-18 (2003).

Wang X., Castillo L. and Araya G., Temperature profiles in forced convection turbulent boundary layers, Journal of Heat Transfer, Vol.130, 2, 2008.

Warhaft Z., Passive scalars in turbulent flows, Annual Review of Fluid Mechanics, Vol. 32: 203-240 (2000).

White, F. M. 1974 Viscous Fluid Flow, 1st edn. McGraw-Hill.

Whiting C.H. and Jansen K.E., A Stabilized finite element method for the incompressible Navier-Stokes equations using a hierarchical basis, International Journal of Numerical Methods in Fluids, 35 (1): 93-116 (2001).

Wu X. and Moin P., Transitional and turbulent boundary layer with heat transfer, Physics of Fluids, 22, 085105, 2010.